Self-Assembled Wigner Crystals as Mediators of Spin Currents and Quantum Information

Bobby Antonio,[1] Abolfazl Bayat,[1] Sanjeev Kumar,[2,3] Michael Pepper,[2,3] and Sougato Bose[1]
[1]Department of Physics and Astronomy, University College London, Gower Street, London WC1E 6BT, United Kingdom
[2]Department of Electronic and Electrical Engineering, University College London, London WC1E 7JE, United Kingdom
[3]London Centre for Nanotechnology, 17-19 Gordon Street, London WC1H 0AH, United Kingdom
(Received 14 July 2015; published 20 November 2015)

Technological applications of many-body structures that emerge in gated devices under minimal control are largely unexplored. Here we show how emergent Wigner crystals in a semiconductor quantum wire can facilitate a pivotal requirement for a scalable quantum computer, namely, transmitting quantum information encoded in spins faithfully over a distance of micrometers. The fidelity of the transmission is remarkably high, faster than the relevant decohering effects, independent of the details of the spatial charge configuration in the wire, and realizable in dilution refrigerator temperatures. The transfer can evidence near unitary many-body nonequilibrium dynamics hitherto unseen in a solid-state device. It could also be useful in spintronics as a method for pure spin current over a distance without charge movement.

DOI: 10.1103/PhysRevLett.115.216804 PACS numbers: 73.21.Hb, 73.21.La, 73.63.Kv, 73.63.Nm

Introduction.—Spin chains can facilitate several important technological applications such as pure spin currents in nonitinerant systems [1], quantum state transfer [2,3], and quantum gates [4–6]. Most of the above applications are facilitated by a nearly unitary dynamics of the spin chain. Such dynamics is not only interesting for potential quantum technology [7,8] but also fundamentally important to address questions of equilibration, quantum thermodynamics, and information propagation [9]. Thus, the physical realization of artificial spin chains that have the potential for long time unitary dynamics is an important quest—they have been realized only very recently, and exclusively in atomic physics systems: in cold atom systems [10,11], ion traps [12,13] and Rydberg systems [14]. In the realm of solid state, on the other hand, nonequilibrium dynamics of engineered spin chains is far from unitary and primarily driven by relaxation [15]. Although some bulk magnetic materials [16,17], nitrogen vacancy center chains [4,6], and Josephson junction arrays [18] hold the potential for long chain unitary dynamics, that is still somewhat distant from experimental realization. As far as the semiconductor realm is concerned, permanently fabricated spin chain structures with dangling bonds [19] or phosphorus dopants [20] may also hold the potential, but is yet to be examined either theoretically or experimentally. A natural question is thus whether one can realize spin chains exhibiting nearly unitary nonequilibrium dynamics in a feasible manner in a two-dimensional electron gas (2DEG) and thereby open the door to the aforementioned applications in solid state.

Individual electrons trapped in gate defined quantum dot arrays have been proposed for simulating spin chains in the limit of one electron in each dot [21]. Although the fabrication of large quantum dot arrays is an active current effort [22,23] and the complex electronics for gate addressing is also being designed [23], it is worth considering the potential of simpler gated structures. In particular, self-assembled charge configurations, such as Wigner crystals, are naturally formed without demanding local control. By controlling the density of electrons one can vary the distance between the charges and consequently engineer their exchange interactions. This, in comparison with quantum dot arrays, allows for stronger exchange couplings which then potentially provide more thermal stability, faster dynamics, and less sensitivity to decoherence.

Here we show that emergent "self-assembled" electronic spin chains arising due to Wigner Crystallization in quasi-1D nanowires can be probed with two spatially separated accessible interfaces (two quantum dots) so that nonequilibrium dynamics and its applications can be probed. Particularly we show how this setting can be used to transfer spin qubits between two quantum dots separated by μm scales, which is currently being actively considered as an important problem, with very few suggested solutions [24–27]. Additionally we suggest a feasible way of observing this phenomenon through pA scale currents, which, in turn, opens up a new option in low dissipation spintronics for a spin current without a charge current.

Wigner crystalization.—By applying strong confining potentials on a 2DEG one may trap a few electrons in a quasi-1D region and effectively make a nanowire. In such nanowires, when the electron density is below a critical value, the Coulomb interactions between electrons overtakes their kinetic energies resulting in a quasi-1D Wigner crystal in which the electrons are extremely localized near to the classical equilibrium configurations. In quasi-1D nanowires where the electrons are strongly confined in two directions, a

Wigner crystal is predicted to emerge when the average electron-electron distance is greater than $4a_B$, where a_B is the Bohr radius [28].

Model.—We consider trapping N electrons (with N even) in a quasi-1D region by using surface electrodes over a 2DEG in GaAs. The trapping potential is modeled as

$$V_{\mathrm{TR}}(x,y) = \frac{1}{2}m^*\Omega^2 y^2 + h_0\left(e^{-[(x-d/2)^2/2w_{\mathrm{out}}^2]} + e^{-[(x+d/2)^2/2w_{\mathrm{out}}^2]}\right)$$

where m^* is the electron effective mass, Ω is the strength of the transverse potential, and the two Gaussian potentials with height h_0 and width w_{out} define a nanowire of length d extending between $x = \pm d/2$. Two small quantum dots, for trapping single electrons, are formed at both ends of the wire by applying proper voltages to the gates. The quantum dots are modeled by the following potential:

$$V_{\mathrm{QD}}(x,y) = h_b\left(e^{-[(x+d/2-l)^2/2w^2]} + e^{-[(x-d/2+l)^2/2w^2]}\right) + \frac{1}{2}m^*\Lambda^2(e^{-[(x-x_0)^2/2\sigma^2]}(y-y_0)^2 + e^{-[(x+x_0)^2/2\sigma^2]}(y+y_0)^2),$$

where the first two Gaussian potentials with heights h_b and width w, centered at the distance l from the boundaries of the wire, create two quantum dots at both sides of the nanowire and the potentials in the second line break the mirror symmetry by displacing the minima in the two quantum dots in opposite directions. The symmetry broken system will have a single equilibrium position for electrons and thus numerical convergence is easier to reach. Choosing appropriate values of the parameters x_0, y_0, and σ is discussed in the Supplemental Material [29] (which includes extra Refs. [30–34]).

We consider $N = 10$ electrons trapped over a distance $d = 1.25$ μm, such that the quantum dots confine one electron each and the remaining eight electrons are placed in the wire as shown in Fig. 1(a). The whole potential is

$$V(\mathbf{R}) = \sum_{k=1}^{N}\left[V_{\mathrm{TR}}(\mathbf{r}_k) + V_{\mathrm{QD}}(\mathbf{r}_k) + \sum_{j<k}\frac{e^2}{4\pi\epsilon|\mathbf{r}_k - \mathbf{r}_j|}\right].$$

The barrier h_b is varied from 3 meV to 50 μeV to decouple or couple the quantum dots to the wire, respectively. Thus, the two endmost electrons can act as sender and receiver when sending quantum information through the chain. Unlike the middle electrons, we assume full control over these two end electrons for initialization and measurement.

Exchange couplings.—At low temperatures the dynamics of the Wigner crystal is approximately governed by the multi-spin-exchange (MSE) Hamiltonian [35]. To calculate the exchange couplings in this Hamiltonian we exploit the semiclassical path integral instanton method [36–40]. This approach is applicable for the regimes where the quantum effects are small, like the case for Wigner crystals where the electrons are well separated [41] (see the Supplemental Material [29] for more details). While our methodology assumes a closed system it is potentially amenable to extension to directly incorporate an environment following the methodology of Ref. [42].

Using the instanton method, it was found that only processes involving up to fourth-nearest neighbor pairwise exchange and up to 4-body exchange were significant. With this restriction, the full spin Hamiltonian can be written (see Supplemental Material for the details [29])

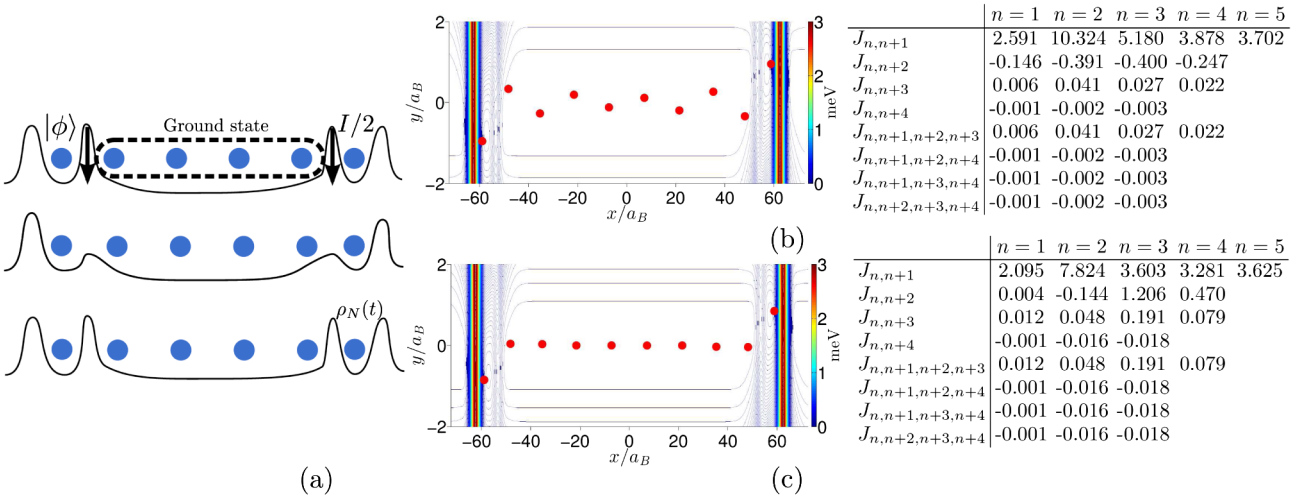

	$n=1$	$n=2$	$n=3$	$n=4$	$n=5$
$J_{n,n+1}$	2.591	10.324	5.180	3.878	3.702
$J_{n,n+2}$	-0.146	-0.391	-0.400	-0.247	
$J_{n,n+3}$	0.006	0.041	0.027	0.022	
$J_{n,n+4}$	-0.001	-0.002	-0.003		
$J_{n,n+1,n+2,n+3}$	0.006	0.041	0.027	0.022	
$J_{n,n+1,n+2,n+4}$	-0.001	-0.002	-0.003		
$J_{n,n+1,n+3,n+4}$	-0.001	-0.002	-0.003		
$J_{n,n+2,n+3,n+4}$	-0.001	-0.002	-0.003		

	$n=1$	$n=2$	$n=3$	$n=4$	$n=5$
$J_{n,n+1}$	2.095	7.824	3.603	3.281	3.625
$J_{n,n+2}$	0.004	-0.144	1.206	0.470	
$J_{n,n+3}$	0.012	0.048	0.191	0.079	
$J_{n,n+4}$	-0.001	-0.016	-0.018		
$J_{n,n+1,n+2,n+3}$	0.012	0.048	0.191	0.079	
$J_{n,n+1,n+2,n+4}$	-0.001	-0.016	-0.018		
$J_{n,n+1,n+3,n+4}$	-0.001	-0.016	-0.018		
$J_{n,n+2,n+3,n+4}$	-0.001	-0.016	-0.018		

FIG. 1 (color online). (a) Transfer protocol for an even number of electrons in which h_b changes from 3 meV to 50 μeV instantaneously to induce dynamics. (b) Classical ground state equilibrium positions for ten electrons with $\Omega = 550$ $\mu\mathrm{eV}/\hbar$. Coupling parameters (in the unit of μeV) are shown for the different 2- and 4-body exchange processes. Since the couplings are symmetric, only half of each coupling is given. (c) Similarly to (b), with $\Omega = 440$ $\mu\mathrm{eV}/\hbar$.

$$H = \sum_{r=1}^{4} \sum_{n=1}^{N-r} J_{n,n+r} \boldsymbol{\sigma}_n \cdot \boldsymbol{\sigma}_{n+r} + \sum_{j<k<l<m} J_{jklm} \Upsilon_{jklm}, \quad (1)$$

where $\boldsymbol{\sigma}_n = (\sigma_n^x, \sigma_n^y, \sigma_n^z)$ is the Pauli vector acting on site n and $\Upsilon_{jklm} := (\boldsymbol{\sigma}_j \cdot \boldsymbol{\sigma}_k)(\boldsymbol{\sigma}_l \cdot \boldsymbol{\sigma}_m) + (\boldsymbol{\sigma}_j \cdot \boldsymbol{\sigma}_m)(\boldsymbol{\sigma}_k \cdot \boldsymbol{\sigma}_l) - (\boldsymbol{\sigma}_j \cdot \boldsymbol{\sigma}_l)(\boldsymbol{\sigma}_k \cdot \boldsymbol{\sigma}_m)$. Exchange couplings for $\Omega = 550\,\mu\text{eV}/\hbar$ and $\Omega = 440\ \mu\text{eV}/\hbar$ are given in units of μeV in the tables next to each charge configurations of Figs. 1(b) and 1(c). The general features are low couplings at the boundary (due to the barrier between the dots and the chain) and a U-shaped coupling along the chain. The next-nearest neighbor couplings are always ferromagnetic (i.e., $J_{n,n+2} < 0$) for the linear configuration while for the zig-zag geometry they show a more complex pattern varying from negative to positive values. The U-shaped feature of the couplings is because the off-center electrons are pushed towards the boundaries due to an unbalanced Coulomb repulsion from the majority of electrons on the opposite side. This makes the effective distance between the electrons shorter in the boundaries and thus results in stronger couplings.

Quantum communication.—We assume that the quantum dots are initially decoupled from the wire (i.e., h_b is large). Furthermore, we consider zero temperature so that the electrons are confined to their lowest vibrational mode and are prepared in their spin ground state $|\text{GS}\rangle$. The electron in one quantum dot is prepared in an arbitrary quantum spin state $|\psi\rangle = \cos(\theta/2)|\uparrow\rangle + e^{i\phi} \sin\theta/2|\downarrow\rangle$, which is supposed to be transferred to the opposite dot, which confines an electron in unpolarized mixed state $I/2$. The initial state of the system is thus $\rho(0) = |\psi\rangle\langle\psi| \otimes |\text{GS}\rangle\langle\text{GS}| \otimes I/2$. The barriers are then simultaneously lowered (i.e., h_b is lowered) in order to start a unitary dynamics under the action of the new Hamiltonian. One can compute the density matrix of the last electron $\rho_N(t)$ by tracing out the others. To quantify the quality of transfer one can compute the fidelity $F(t) = \langle\psi|\rho_N(t)|\psi\rangle$ which is independent of θ and ϕ due to the SU(2) symmetry of the Hamiltonian.

In Figs. 2(a) and 2(b) we plot $F(t)$ as a function of time for the two charge configurations with $\Omega = 550\ \mu\text{eV}/\hbar$ (linear chain) and $\Omega = 440\ \mu\text{eV}/\hbar$ (zig-zag chain). It is clear from these figures that the fidelity peaks at a time $t = t_m$ and the takes its maximum value $F_{\max} = F(t_m)$. Although the linear chain gives a faster dynamics with $t_m \simeq 4$ ns (due to fairly larger couplings) in comparison with the zig-zag charge configuration with $t_m \simeq 8$ ns, the maximum fidelity $F_{\max}$ is remarkably high for both configurations, certainly larger than a uniform chain [43]. These results illustrate the key point that the details of the charge configurations are not important for the quality of spin transport. To see the scalability, we plot $F_{\max}$ as a function of N in Fig. 2(c), keeping the density of electrons fixed and using only nearest-neighbor couplings since these are by far the largest and computing higher order interactions

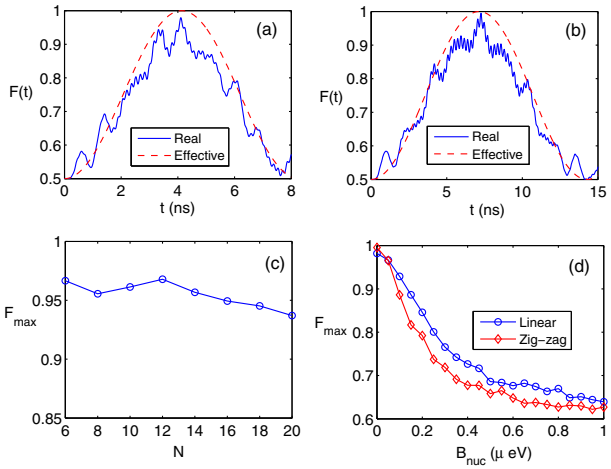

FIG. 2 (color online). Average fidelity F_{av} as a function of time, when h_b suddenly changes from 3 meV to 50μeV, using both real and effective Hamiltonians for: (a) the linear chain ($\Omega = 550\ \mu\text{eV}/\hbar$); and (b) the zig-zag chain ($\Omega = 440\ \mu\text{eV}/\hbar$). (c) $F_{\max}$ versus N. (d) The variation in $F_{\max}$ when a random magnetic field of variance B_{nuc} is included in the Hamiltonian.

becomes computationally prohibitive for > 10 electrons. As the figures show the fidelity $F_{\max}$ remains very high even for chains up to $N = 20$ electrons.

Explanation.—To understand the remarkably high fidelities achieved through the time evolution of the Wigner crystal, one has to consider the nearest-neighbor couplings, which dominate the Hamiltonian H. As shown in the tables in Figs. 1(b) and 1(c), the couplings $J_{2,3}$ (which are identical to $J_{N-2,N-1}$) are almost 4 times stronger than the couplings $J_{1,2}$ (which are identical to $J_{N-1,N}$) in both charge configurations. This implies that the ground state and first excited state of the Hamiltonian H show delocalized strong correlations between the boundary electrons. By computing the reduced density matrix of the two ending spins ρ_{1N} from the ground state of H one can see that $\langle\psi^-|\rho_{1,N}|\psi^-\rangle > 0.8$, where $|\psi^-\rangle$ is the singlet state, for both charge configurations. Similarly, by computing ρ_{1N} from the first excited state of H one gets $\langle\psi^+|\rho_{1,N}|\psi^+\rangle > 0.9$, where $|\psi^+\rangle$ is the triplet state. The delocalized eigenvectors of the Hamiltonian create an effective RKKY-like interaction between the two boundary electrons in the dots [44,45], namely, $H_{\text{eff}} = J_{\text{eff}} \boldsymbol{\sigma}_1 \cdot \boldsymbol{\sigma}_N$ where $J_{\text{eff}} = \Delta E/4$ in which ΔE stands for the energy gap of the Hamiltonian H. In Figs. 2(a) and 2(b) the time evolution of average fidelities using both H_{eff} and H are plotted which shows that the effective Hamiltonian can qualitatively explain the real dynamics of the system. In fact, the effective model becomes more precise by decreasing the boundary couplings J_{12} and $J_{N-1,N}$.

Imperfections.—So far, we have assumed that the system operates at zero temperature and thus the electrons in the wire are initialized in their ground state. In order to guarantee that the proposed protocol remains valid at finite

temperature T, one has to satisfy $k_B T < \Delta E$, where k_B is the Boltzmann constant. For the given set of couplings the energy gaps are $\Delta E \simeq 0.77$ μeV for the linear and $\Delta E \simeq 0.45$ μeV for the zig-zag configurations giving the range of temperature as $k_B T \sim 5$–10 mK which can be achieved in current dilution refrigerators [46].

In GaAs heterostructures the electron spins interact with the nuclear spins of the host material. Because of the very slow dynamics of nuclei spins in comparison to the time scales of our protocol one can describe their average effect on electron spin n as an effective random magnetic field $\hat{\mathbf{B}}_n$. While the direction of this field is fully random its amplitude has a Gaussian distribution [47]

$$P(\hat{\mathbf{B}}) = \exp[-\hat{\mathbf{B}} \cdot \hat{\mathbf{B}}/2B_{\mathrm{nuc}}^2]/(2\pi B_{\mathrm{nuc}}^2)^{3/2}, \qquad (2)$$

in which $3B_{\mathrm{nuc}}^2$ is the variance of the distribution. The total Hamiltonian thus changes as

$$H \to H + \sum_{n=1}^{N} \hat{\mathbf{B}}_n . \boldsymbol{\sigma}_k. \qquad (3)$$

In Fig. 2(d) we plot the maximum fidelity F_{max} versus B_{nuc} which shows the destructive effect of the hyperfine interaction. The linear configuration performs better for larger values of B_{nuc} since the faster dynamics reduces the time exposed to nuclear spins. A realistic value for B_{nuc} is 2–6 mT (i.e., ~0.07–0.23 μeV) [48], at which the fidelity of $F_{\mathrm{max}} \simeq 0.8$–$0.95$ is attainable. Using spin-orbit coupling one may effectively suppress B_{nuc} to 35 neV [49].

At experimental temperatures (~50 mK) thermal phonons are absent in the material [50]. Moreover, the bulk phonon wavelengths (~μm) exceed electron wavelengths (~20 nm) so much that the electrons do not couple to them either. However, sudden quench in h_b may cause the electrons to jiggle around their positions causing fluctuations in exchange interactions. As shown in the Supplemental Material [29], these high frequency vibrations ($f \simeq 100$ GHz) are integrated out during the transmission time $t_m \simeq 5$ ns.

Experimental realization.—The quantum dot-quantum wire-quantum dot system can be realized in a III-V material such as GaAs/AlGaAs heterostructure [51], using gates and the quantum point contacts technique, as shown in Fig. 3. We assume that the quantum wire has achieved a state of Wigner crystallization [52]. Spin initialization in the left dot and read-out in the right dot after the transfer time, can be performed using demonstrated techniques [48,53] such as singlet-triplet charge measurements by appending double dots to both ends of the wire. However, here we show how transport measurements can also probe our mechanism by effectively detecting the transfer of a spin current. The prototype of this measurement consists of a left electron pump [54–56] injecting polarized electrons (say, from a standard source [51,57]) whereas the right pump injects unpolarized electrons in the respective

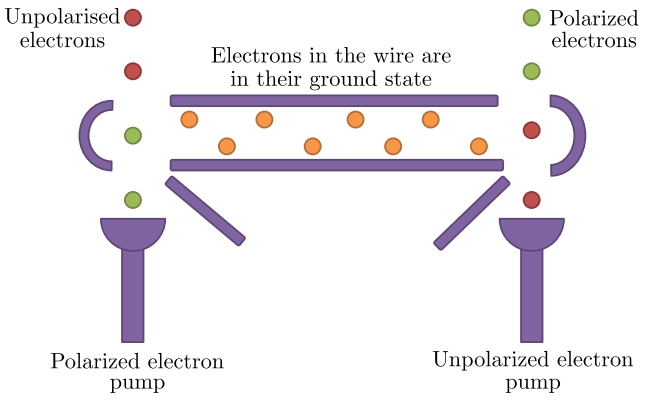

FIG. 3 (color online). Schematic diagram of a possible physical implementation of the mechanism in GaAs. Polarized electrons (green circles) are pumped into the left quantum dot, while unpolarized electrons (red circles) are pumped into the right dot. Interaction with the confined electrons in the wire (orange circles) swaps the electron spins and thus exchanges the polarization of the currents. A spin polarisation measurement on the output current can detect the transfer of polarized electrons.

quantum dots as shown in Fig. 3. As the electrons are injected into the dots they interact with the electrons in the quantum wire as the barrier height is reduced and their quantum state is swapped. Thus upon exiting the dots, the initially polarized electrons will be unpolarized and vice-versa. As the interaction time for spin swap is about $t_m \sim 4$ ns ($t_m \sim 8$ ns) for the linear (zig-zag) configuration the electrons must stay in the dot for such time. This implies that the pumps have to inject a current of 20 pA–40 pA depending on the configuration of electrons in the quantum wire. A spin polarization of the current carried off from the right dot by the right pump could then be detected by the halving of the conductance through a quantum point contact in series with the right dot.

Discussion and conclusions.—We have shown that entirely within the remit of gate defined structures, one can use a Wigner crystal in a quantum wire for transferring spin qubits between quantum dots separated by micrometers reaching very high fidelities. Compared to varied proposals for mediating between separated quantum dot spin qubits [24–27], the proposed mechanism can have various advantages. For example, it could have higher speed making it more resilient to decoherence, simpler fabrication compared to hybrid systems, and a greater spatial extension over few electron quantum dot mediators. Furthermore, thanks to the self-assembled nature of the Wigner crystal, our scheme does not require complex electronics to artificially create a regular structure of exchange coupled spins. Our analysis shows the proposed protocol can operate in current dilution refrigerators, and remarkably the details of the charge configuration does not influence the performance of the system, adding additional robustness to the device fabrication. It also opens an avenue in spintronics by facilitating the spatial transport of a spin

current without a charge current, and provides a smoking gun for the near unitary nonequilibrium dynamics in many-body solid-state systems. Alternative realizations of Wigner crystals, in liquid helium [58], ion traps [59], and carbon nanotubes [60], can also be used for implementing our mechanism.

The authors thank Martin Uhrin for illuminating discussions on use of the 2-point steepest descent algorithm. This work was supported by the Engineering and Physical Sciences Research Council (EPSRC), UK. The research leading to these results has received funding from the European Research Council under the European Union's Seventh Framework Programme (FP/2007-2013)/ERC Grant Agreement No. 308253.

[1] K. A. van Hoogdalem and D. Loss, Phys. Rev. B **84**, 024402 (2011).
[2] S. Bose, Contemp. Phys. **48**, 13 (2007).
[3] G. M. Nikolopoulos and I. Jex, *Quantum State Transfer and Network Engineering* (Springer, New York, 2013).
[4] N. Y. Yao, L. Jiang, A. V. Gorshkov, Z.-X. Gong, A. Zhai, L.-M. Duan, and M. D. Lukin, Phys. Rev. Lett. **106**, 040505 (2011).
[5] L. Banchi, A. Bayat, P. Verrucchi, and S. Bose, Phys. Rev. Lett. **106**, 140501 (2011).
[6] M. Schaffry, S. C. Benjamin, and Y. Matsuzaki, New J. Phys. **14**, 023046 (2012).
[7] A. Bayat, S. Bose, and P. Sodano, Phys. Rev. Lett. **105**, 187204 (2010).
[8] Z.-M. Wang, R.-S. Ma, C. A. Bishop, and Y.-J. Gu, Phys. Rev. A **86**, 022330 (2012).
[9] C. Gogolin and J. Eisert, arXiv:1503.07538.
[10] T. Fukuhara, P. Schauß, M. Endres, S. Hild, M. Cheneau, I. Bloch, and C. Gross, Nature (London) **502**, 76 (2013).
[11] T. Fukuhara, S. Hild, J. Zeiher, P. Schauß, I. Bloch, M. Endres, and C. Gross, Phys. Rev. Lett. **115**, 035302 (2015).
[12] P. Richerme, Z.-X. Gong, A. Lee, C. Senko, J. Smith, M. Foss-Feig, S. Michalakis, A. V. Gorshkov, and C. Monroe, Nature (London) **511**, 198 (2014).
[13] P. Jurcevic, B. P. Lanyon, P. Hauke, C. Hempel, P. Zoller, R. Blatt, and C. F. Roos, Nature (London) **511**, 202 (2014).
[14] D. Barredo, H. Labuhn, S. Ravets, T. Lahaye, A. Browaeys, and C. S. Adams, Phys. Rev. Lett. **114**, 113002 (2015).
[15] A. A. Khajetoorians, J. Wiebe, B. Chilian, and R. Wiesendanger, Science **332**, 1062 (2011).
[16] S. Sahling, G. Remenyi, C. Paulsen, P. Monceau, V. Saligrama, C. Marin, A. Revcolevschi, L. Regnault, S. Raymond, and J. Lorenzo, Nat. Phys. **11**, 255 (2015).
[17] C. Mitra, Nat. Phys. **11**, 212 (2015).
[18] U. L. Heras, A. Mezzacapo, L. Lamata, S. Filipp, A. Wallraff, and E. Solano, Phys. Rev. Lett. **112**, 200501 (2014).
[19] R. A. Wolkow, L. Livadaru, J. Pitters, M. Taucer, P. Piva, M. Salomons, M. Cloutier, and B. V. Martins, in *Field-Coupled Nanocomputing* (Springer, New York, 2014) pp. 33–58.
[20] F. A. Zwanenburg, A. S. Dzurak, A. Morello, M. Y. Simmons, L. C. Hollenberg, G. Klimeck, S. Rogge, S. N. Coppersmith, and M. A. Eriksson, Rev. Mod. Phys. **85**, 961 (2013).
[21] C. A. Stafford and S. Das Sarma, Phys. Rev. Lett. **72**, 3590 (1994).
[22] P. Barthelemy and L. M. Vandersypen, Ann. Phys. (Berlin) **525**, 808 (2013).
[23] R. Puddy, L. Smith, H. Al-Taie, C. Chong, I. Farrer, J. Griffiths, D. Ritchie, M. Kelly, M. Pepper, and C. Smith, Appl. Phys. Lett. **107**, 143501 (2015).
[24] L. Trifunovic, O. Dial, M. Trif, J. R. Wootton, R. Abebe, A. Yacoby, and D. Loss, Phys. Rev. X **2**, 011006 (2012).
[25] L. Trifunovic, F. L. Pedrocchi, and D. Loss, Phys. Rev. X **3**, 041023 (2013).
[26] S. Mehl, H. Bluhm, and D. P. DiVincenzo, Phys. Rev. B **90**, 045404 (2014).
[27] V. Srinivasa, H. Xu, and J. M. Taylor, Phys. Rev. Lett. **114**, 226803 (2015).
[28] R. Egger, W. Häusler, C. H. Mak, and H. Grabert, Phys. Rev. Lett. **82**, 3320 (1999).
[29] See Supplemental Material at http://link.aps.org/supplemental/10.1103/PhysRevLett.115.216804 for more details on trapping potentials and computing the exchange couplings.
[30] K. Voelker and S. Chakravarty, Phys. Rev. B **64**, 235125 (2001).
[31] M. Katano and D. S. Hirashima, Phys. Rev. B **62**, 2573 (2000).
[32] J. O. Richardson and S. C. Althorpe, J. Chem. Phys. **134**, 054109 (2011).
[33] D. Klein, J. Phys. A **13**, 3141 (1980).
[34] J. Barzilai and J. M. Borwein, IMA J. Numer. Anal. **8**, 141 (1988).
[35] D. J. Thouless, Proc. Phys. Soc. London **86**, 893 (1965).
[36] M. Roger, J. H. Hetherington, and J. M. Delrieu, Rev. Mod. Phys. **55**, 1 (1983).
[37] D. S. Hirashima and K. Kubo, Phys. Rev. B **63**, 125340 (2001).
[38] A. D. Klironomos, R. R. Ramazashvili, and K. A. Matveev, Phys. Rev. B **72**, 195343 (2005).
[39] A. D. Klironomos, J. S. Meyer, T. Hikihara, and K. A. Matveev, Phys. Rev. B **76**, 075302 (2007).
[40] J. Meyer and K. Matveev, J. Phys. Condens. Matter **21**, 023203 (2009).
[41] B. Bernu, L. Cândido, and D. M. Ceperley, Phys. Rev. Lett. **86**, 870 (2001).
[42] D. Segal, A. J. Millis, and D. R. Reichman, Phys. Rev. B **82**, 205323 (2010).
[43] A. Bayat and S. Bose, Phys. Rev. A **81**, 012304 (2010).
[44] L. Campos Venuti, S. M. Giampaolo, F. Illuminati, and P. Zanardi, Phys. Rev. A **76**, 052328 (2007).
[45] M. Friesen, A. Biswas, X. Hu, and D. Lidar, Phys. Rev. Lett. **98**, 230503 (2007).
[46] G. Batey, A. Casey, M. Cuthbert, A. Matthews, J. Saunders, and A. Shibahara, New J. Phys. **15**, 113034 (2013).
[47] J. M. Taylor, J. R. Petta, A. C. Johnson, A. Yacoby, C. M. Marcus, and M. D. Lukin, Phys. Rev. B **76**, 035315 (2007).
[48] A. Johnson, J. Petta, J. Taylor, A. Yacoby, M. Lukin, C. Marcus, M. Hanson, and A. Gossard, Nature (London) **435**, 925 (2005).
[49] J. M. Nichol, S. P. Harvey, M. D. Shulman, A. Pal, V. Umansky, E. I. Rashba, B. I. Halperin, and A. Yacoby, Nat. Commun. **6**, 7682 (2015).
[50] P. V. E. McClintock, D. J. Meredith, and J. K. Wigmore, *Low-Temperature Physics* (Springer, New York, 1992).

[51] H. Kosaka, A. A. Kiselev, F. A. Baron, K. W. Kim, and E. Yablonovitch, Electron. Lett. **37**, 464 (2001).
[52] J. S. Meyer, K. A. Matveev, and A. I. Larkin, Phys. Rev. Lett. **98**, 126404 (2007).
[53] M. D. Shulman, O. E. Dial, S. P. Harvey, H. Bluhm, V. Umansky, and A. Yacoby, Science **336**, 202 (2012).
[54] M. Blumenthal, B. Kaestner, L. Li, S. Giblin, T. Janssen, M. Pepper, D. Anderson, G. Jones, and D. Ritchie, Nat. Phys. **3**, 343 (2007).
[55] T. Nakaoka, T. Saito, J. Tatebayashi, S. Hirose, T. Usuki, N. Yokoyama, and Y. Arakawa, Phys. Rev. B **71**, 205301 (2005).
[56] S. Kumar, K. J. Thomas, L. W. Smith, M. Pepper, G. L. Creeth, I. Farrer, D. Ritchie, G. Jones, and J. Griffiths, Phys. Rev. B **90**, 201304 (2014).
[57] R. Harrell, K. Pyshkin, M. Simmons, D. Ritchie, C. Ford, G. Jones, and M. Pepper, Appl. Phys. Lett. **74**, 2328 (1999).
[58] P. M. Platzman and M. I. Dykman, Science **284**, 1967 (1999).
[59] J. D. Baltrusch, A. Negretti, J. M. Taylor, and T. Calarco, Phys. Rev. A **83**, 042319 (2011).
[60] V. V. Deshpande and M. Bockrath, Nat. Phys. **4**, 314 (2008).